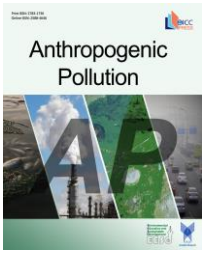

Anthropog Pollut 2026; 10(1): 172-185

Anthropogenic Pollution (AP)

https://doi.org/10.57647/AP.2026.1001.12

Research Article

Electrodeposited CdS Nanostructured Thin Films as a Photoelectrochemical Sensor for Monitoring Pb(II) in Aquatic Environments

Zahra Ghalandari Qojlu[1], Nasim Nobari[1,*], Mahdi Behboudnia[2]

[1] *Department of Physics, Mah.C., Islamic Azad University, Mahabad, Iran*
[2] *Department of Physics, Urmia University of Technology, P.O. Box 57155-419, Urmia, Iran*

***Corresponding author:** nasimnobari@iau.ac.ir

Article History:

Received:
10 May 2026

Revised:
15 June 2026

Accepted:
25 June 2026

Published in Issue:
30 June 2026

Abstract

Nanostructured CdS thin films were fabricated on FTO substrates by electrodeposition for the photoelectrochemical detection of Pb (II) ions in water. The CdS films were deposited at an applied potential of 830 mV for 6 min, producing uniform nanostructured coatings on the conductive substrate. The structural, morphological, and compositional characteristics of the films were systematically investigated using X ray diffraction (XRD), scanning electron microscopy (SEM), and energy dispersive X ray spectroscopy (EDS). XRD analysis confirmed the formation of polycrystalline CdS with well-defined diffraction peaks corresponding to the CdS phase. SEM observations revealed a homogeneous nanostructured surface composed of closely packed grains with an average size of approximately 40 nm, providing a high surface area beneficial for sensing applications. EDS spectra verified the presence of Cd and S as the dominant elements, indicating the successful formation of CdS without detectable impurity phases. Optical characterization indicated a band gap energy of approximately 3.3 eV, demonstrating suitable photoactive behavior under visible light illumination. The photoelectrochemical sensing performance of the CdS thin films toward Pb (II) ions was evaluated in the concentration range of 1–20 ppm under periodic illumination (10 s light/dark cycles). The photocurrent response increased linearly with increasing Pb (II) concentration, following the calibration relationship:

$$I(\mu A) = 0.42C + 0.19$$

The stronger sensing response is mainly due to the nanostructured CdS surface, which helps separate charges more efficiently and offers more sites for Pb (II) to bind. Overall, electrodeposited CdS films provide a simple, affordable, and effective way to detect Pb (II) in water.

Keywords: CdS thin films; Nanostructured photoelectrodes; Pb(II) quantification; Potentially toxic elements (PTEs); Aquatic environment monitoring

Cite this article: Ghalandari Qojlu, Z., Nobari, N.,& Behboudnia, M.(2026). Electrodeposited CdS Nanostructured Thin Films as a Photoelectrochemical Sensor for Monitoring Pb(II) in Aquatic Environments. *Anthropogenic Pollution, 10(1),* 172-185. https://doi.org/10.57647/AP.2026.1001.12

1. Introduction

Contamination of aquatic environments by potentially toxic elements (PTEs) has become a major environmental and public health concern due to their persistence, toxicity, and ability to bioaccumulate in living organisms. These elements can accumulate in water bodies through natural processes as well as anthropogenic activities such as mining, industrial discharge, and agricultural runoff, posing serious risks to ecosystems and human health (Edo et al., 2024; Mousavi Moghanjooghi et al., 2022).

In recent years, nanostructured materials have attracted considerable attention because of their unique physical and chemical properties, which differ significantly from those of their bulk counterparts. These distinctive characteristics arise from quantum confinement effects, reduced dimensionality, and an increased surface-to-volume ratio, which strongly influence the optical and electronic behavior of materials at the nanoscale. As a result, semiconductor nanostructures have been widely investigated for applications in nanoelectronics, photonics, optoelectronic devices, and sensing technologies (Lieber & Wang, 2007; Pan, Dai, & Wang, 2001). In particular, wide-bandgap semiconductor nanomaterials exhibit remarkable optical and charge-transport properties, making them promising candidates for energy conversion systems, environmental monitoring, sensing technologies, and advanced electronic applications (Minnich, Dresselhaus, Ren, & Chen, 2009; Sootsman, Chung, & Kanatzidis, 2009).

One of the most important characteristics of semiconductor nanostructures is their photosensitivity, which enables the conversion of incident light into measurable electrical signals. When illuminated with photons possessing energy equal to or greater than the band gap of the semiconductor, electron–hole pairs are generated within the material, leading to an increase in charge carrier concentration and enhanced electrical conductivity (Lieber & Wang, 2007; Pan et al., 2001). This photoinduced electrical response forms the fundamental operating mechanism of photodetectors, photovoltaic devices, optical sensors, and photoelectrochemical (PEC) systems (Logeeswaran et al., 2011; Mondal & Ray, 2009; Zhai et al., 2010; Qiu & Tang, 2020). Compared with conventional electrochemical sensing approaches, PEC sensors offer several advantages, including high sensitivity, low background signal, rapid response, and efficient operation under visible-light irradiation, making them highly attractive for environmental monitoring applications.

Alongside their technological importance, semiconductor nanostructures have recently attracted considerable attention for environmental sensing applications, particularly for the detection of potentially toxic elements (PTEs) in aquatic systems. PTEs are persistent and non-biodegradable pollutants that can accumulate in aquatic organisms and subsequently enter the food chain, posing serious ecological and human-health risks. Industrial discharge, petrochemical activities, mining operations, and municipal wastewater have significantly increased PTE pollution in both marine and freshwater environments. Studies conducted in the Persian Gulf region have reported considerable accumulation of cadmium and arsenic in marine organisms such as the crab Portunus pelagicus collected from the Asalouyeh coastal area (Fatemi & Khoramnejadian, 2016). Similarly, investigations of offshore sediments have revealed elevated concentrations of hazardous metals, indicating severe ecological risks in contaminated regions (Aali et al., 2024). Soil-based environmental studies have also demonstrated strong correlations between magnetic susceptibility, PTE concentration, and physicochemical soil properties, further confirming the widespread distribution of metal contamination across different ecosystems (Ghobadi et al., 2024). These findings highlight the urgent need for sensitive, reliable, and cost-effective sensing technologies for monitoring PTEs in aquatic environments.

Among various semiconductor materials, cadmium sulfide (CdS) has attracted considerable attention as a photoactive material for sensing applications due to its direct band gap (~2.4 eV), strong visible-light absorption, and favorable charge-transport properties. These characteristics make CdS nanostructures particularly suitable for photoelectrochemical sensing platforms, where illumination enhances the generation and separation of charge carriers, leading to improved detection sensitivity. In addition, nanostructured CdS thin films provide a large active surface area and efficient interfacial charge transfer, which are advantageous for detecting trace concentrations of metal ions in aqueous environments. Consequently, CdS-based photoelectrodes have been widely explored for environmental monitoring applications, particularly for the detection of toxic metal ions such as Pb(II) in water systems.

Among potentially toxic elements (PTEs), lead ions (Pb^{2+}) are particularly hazardous because of their high toxicity, environmental persistence, and severe adverse effects on the nervous, renal, and developmental systems, even at trace concentrations. Consequently, accurate monitoring of Pb^{2+} in water resources has become an important public health priority (Mitchell et al., 2024). Recent advances in photoelectrochemical (PEC) and optical sensing technologies have demonstrated that semiconductor nanostructures can provide high sensitivity, rapid response, and enhanced photoelectrical performance

10.57647/AP.2026.1001.12

for PTE ion detection. For example, Cao et al. (2021) developed an advanced PEC aptasensor based on CdSe quantum dot co-sensitized ZnO–CdS nanostructures for Pb^{2+} detection. Their signal-off sensing strategy, relying on aptamer–Pb^{2+} interaction and G-quadruplex formation, achieved an ultralow detection limit of 3.4×10−103.4×10−10 M, highlighting the strong potential of semiconductor-based hybrid nanostructures for environmental sensing applications.

However, despite their excellent sensitivity, many previously reported sensing systems involve complex fabrication procedures, expensive materials, multistep synthesis routes, or sophisticated surface functionalization processes. Therefore, the development of simpler, low-cost, and scalable photoresponsive thin-film sensors with reliable performance remains an important research challenge.

In this study, nanostructured CdS thin films were fabricated on FTO substrates using a simple electrodeposition technique with a two-electrode configuration. The prepared films were structurally and morphologically characterized using X-ray diffraction (XRD), scanning electron microscopy (SEM), and energy-dispersive X-ray spectroscopy (EDS). The photoelectrochemical response of the CdS thin films under visible-light illumination was investigated for the detection of Pb^{2+} ions in aqueous solutions. The results demonstrate that the electrodeposited CdS films exhibit a clear and concentration-dependent photocurrent response toward Pb^{2+}, indicating their potential as a simple, low-cost, and effective photoelectrochemical sensor for monitoring lead contamination in aquatic environments.

Among various semiconductor materials, cadmium sulfide (CdS) has attracted significant attention due to its direct band gap, high absorption coefficient in the visible-light region, favorable charge-transport behavior, and good chemical stability. CdS-based nanostructures have been widely investigated for applications in solar cells, thin-film transistors, photodetectors, light-emitting devices, and optical sensing systems because of their efficient photoinduced charge-generation capability (Shan et al., 2005; Jiang et al., 2007). The photosensitivity and optoelectronic performance of CdS thin films strongly depend on several parameters, including band gap energy, crystallinity, grain size, film thickness, and surface morphology. In addition, various semiconductor nanostructures such as CdSe, ZnS_xSe_{1-x}, and solution-processed CdSe nanocrystal films have also been successfully employed in photosensing applications, demonstrating promising optical and electrical properties (Hankare et al., 2006; Patil et al., 2018; Dondapati et al., 2013). These studies highlight the potential of II–VI semiconductor nanostructures for photoresponsive sensing platforms and further motivate the investigation of CdS nanostructured thin films for environmental monitoring applications.

Different techniques have been employed for the fabrication of CdS thin films, including thermal evaporation, chemical vapor deposition, chemical bath deposition, spray pyrolysis, and electrodeposition (Hankare et al., 2006; Patil et al., 2018). Among these methods, electrodeposition offers several important advantages, such as simple operation, low fabrication cost, rapid processing, low-temperature synthesis, and precise control over film thickness, morphology, and grain structure. Furthermore, electrodeposition enables uniform film growth on conductive substrates and is suitable for large-scale fabrication of photoactive thin films. Despite these advantages, relatively limited studies have focused on the application of electrodeposited CdS thin films for the photoelectrochemical detection of potentially toxic element (PTE) ions, particularly Pb^{2+} under visible-light irradiation. To the best of our knowledge, only a few studies have reported the use of electrodeposited CdS nanostructured thin films fabricated through a simple two-electrode approach for visible-light-assisted photoelectrochemical detection of Pb^{2+} ions. Therefore, developing simple and reliable photoresponsive sensing platforms based on semiconductor thin films remains an important research direction.

Therefore, in the present study, nanostructured CdS thin films were fabricated on FTO/glass substrates using a simple and rapid electrodeposition method based on a homemade two-electrode configuration. The structural, morphological, and compositional properties of the prepared films were systematically characterized using X-ray diffraction (XRD), scanning electron microscopy (SEM), and energy-dispersive X-ray spectroscopy (EDS). Furthermore, the photoelectrochemical response of the CdS thin films under visible-light irradiation was investigated for the detection of Pb^{2+} ions in aqueous media. The results demonstrate that the electrodeposited CdS thin films exhibit a clear and concentration-dependent photocurrent response toward Pb^{2+} ions, indicating their potential as simple, efficient, and cost-effective photoelectrochemical sensors for environmental monitoring applications.

2. Material & method

CdS thin films were deposited on fluorine-doped tin oxide (FTO) coated glass substrates using an electrodeposition technique. Cadmium chloride monohydrate ($CdCl_2 \cdot H_2O$, 0.2 M, ≥99% purity, Qualikems Fine Chem Pvt. Ltd., Vadodara, India) and sodium thiosulfate ($Na_2S_2O_3$, 0.02 M, ≥99% purity, Merck, Darmstadt, Germany) were used as

10.57647/AP.2026.1001.12

precursor materials without further purification. All aqueous solutions were prepared using deionized water with a resistivity of 18.2 MΩ·cm at room temperature.

Prior to deposition, the FTO/glass substrates were ultrasonically cleaned sequentially with acetone, ethanol, and deionized water to remove surface contaminants and then dried under ambient conditions. The electrolyte solution was prepared by dissolving $CdCl_2 \cdot H_2O$ and $Na_2S_2O_3$ in deionized water, and the pH of the solution was adjusted to 1.4 using hydrochloric acid (HCl). The electrodeposition process was carried out in a homemade two-electrode electrochemical cell. The FTO/glass substrate served as the cathode, while a high-purity platinum grid was used as the anode. The electrodes were positioned vertically and separated by a distance of approximately 3 cm inside the electrolyte solution. During deposition, the electrolyte temperature was maintained at 80∘C80∘C using a hotplate and continuously monitored with a thermometer to ensure thermal stability throughout the experiment. An adjustable DC power supply operating in the voltage range of 0–25 V with a resolution of 1 mV was employed for the deposition process. CdS thin films were electrodeposited onto the FTO substrate at an applied potential of 830 mV for 6 min. After deposition, the prepared films were thoroughly rinsed with deionized water to remove residual electrolyte species and dried at room temperature. Finally, the deposited CdS thin films were annealed in air at 400∘C for 20 min to improve crystallinity and film adhesion.

2.1. XRD analysis

The crystalline structure and phase composition of the electrodeposited CdS thin films was investigated by X-ray diffraction (XRD) using a Bruker D8 Advance diffractometer (Bruker AXS GmbH, Karlsruhe, Germany) equipped with a Cu Kα radiation source (λ = 1.5406 Å). The instrument was operated at an accelerating voltage of 40 kV and a current of 30 mA. The diffraction patterns were recorded in the 2θ range of 10–60° with a step size of 0.02°.

The crystallite size and lattice strain of the CdS thin films were estimated using the Williamson–Hall (W–H) method according to the following relation:) Williamson & Hall, 1953).

$$\beta\cos\,\theta = \frac{\lambda}{L} + \varepsilon\sin\,\theta$$

where β represents the full width at half maximum (FWHM) of the diffraction peak expressed in radians, λ (1.5406 Å) is the wavelength of Cu Kαα radiation, θ is the Bragg diffraction angle, L is the crystallite size, and ε is the lattice strain. By plotting βcosθ as a function of sinθ, a linear relationship is obtained, where the intercept corresponds to λ/L (from which the crystallite size is calculated) and the slope represents the lattice strain.
The results indicate that the electrodeposited CdS thin films consist of nanocrystalline grains with an average crystallite size of approximately XXX nm, while the calculated lattice strain is XXX.

Furthermore, the interplanar spacing of the (hkl) crystal planes were determined using Bragg's law (Bragg, 1913):

$$2d_{hkl}\,Sin\theta = n\lambda$$

The XRD results were used to evaluate the crystallinity, preferred orientation, and possible secondary phases of the CdS films.

2.2. SEM studies

The surface morphology and microstructural features of the electrodeposited CdS thin films were examined using a field-emission scanning electron microscope (FE-SEM, MIRA3 TESCAN, Brno, Czech Republic). The observations were carried out at an accelerating voltage of 15 kV under high-vacuum conditions.

SEM images were recorded at different magnifications (100 nm, 200 nm, 2 μm, and 10 μm) to evaluate both nanoscale surface features and larger microstructural domains. The samples were introduced directly into the SEM chamber without applying additional conductive coating. All measurements were performed at an accelerating voltage of 15–20 kV with an optimized working distance to obtain high-resolution and well-focused surface images. The obtained micrographs were used to assess surface morphology, grain distribution, and the uniformity of the electrodeposited CdS layer.

2.3. Energy-Dispersive X-ray Spectroscopy (EDS)

The elemental composition of the CdS thin films was investigated using energy-dispersive X-ray spectroscopy (EDS) attached to the FE-SEM system (MIRA3 TESCAN, Brno, Czech Republic). Prior to analysis, the samples were sputter-coated with a thin layer of gold (Au) to improve surface conductivity and imaging stability.

EDS spectra were collected at an accelerating voltage of 15–20 kV. The identification of characteristic peaks and elemental analysis were carried out using standard microanalysis procedures (Ji et al., 2022). The spectra confirmed the presence of cadmium (Cd) and sulfur (S) as the primary constituent elements of the deposited films. The observed Au peaks originated from the sputter-coating layer applied during sample preparation. No additional impurity elements were detected within the instrumental

detection limits. Elemental weight percentages obtained from the EDS analysis were used to verify the chemical composition and stoichiometric nature of the CdS thin films.

2.4. Preparation and Analysis of Pb^{2+}-Containing Water Samples

To evaluate the practical applicability of the fabricated CdS nanostructured thin-film sensor, aqueous samples containing Pb^{2+} ions were prepared and analyzed under laboratory conditions. The Pb^{2+} solutions were prepared by dissolving an appropriate amount of lead nitrate ($Pb(NO_3)_2$) in deionized water. Different concentrations of Pb^{2+} ions, including 2, 5, and 10 ppm, were prepared to simulate lead contamination levels commonly encountered in polluted water environments. The prepared solutions were stirred for several minutes using a magnetic stirrer to ensure uniform distribution of Pb^{2+} ions throughout the solution. All solutions were prepared and analyzed at room temperature.

Sensing measurements were performed using the CdS nanostructured thin-film electrode electrodeposited on an FTO substrate at an applied potential of 830 mV for 6 min. The prepared electrode was immersed in the Pb^{2+}-containing aqueous solutions, and the photocurrent response was recorded under periodic light illumination consisting of 10 s light and 10 s dark cycles. Each measurement was repeated at least three times to ensure reproducibility. The concentration of Pb^{2+} ions was determined based on the calibration equation obtained from the photocurrent response, and the sensing performance of the CdS thin-film electrode was evaluated for the detection of lead ions in aqueous media.

To evaluate the reproducibility of the sensor, each Pb^{2+} measurement was repeated at least three times under identical conditions (10 s light/10 s dark cycles, room temperature). The relative standard deviation (RSD) for triplicate measurements at 5 ppm, 10 ppm, and 15 ppm Pb^{2+} was found to be < 4.5%, indicating good repeatability. Additionally, three independent CdS-coated electrodes were fabricated under the same electrodeposition conditions and tested with 10 ppm Pb^{2+} solution. The inter-electrode RSD was < 6.2%, demonstrating acceptable batch-to-batch reproducibility.

The sensor response remained stable over 5 consecutive measurement cycles with the same electrode, showing < 3% signal drift, which confirms the operational stability of the CdS nanostructured film under the tested conditions.

2.5. Photoelectrochemical Measurements

The photoelectrochemical (PEC) performance of the electrodeposited CdS thin films was investigated using an Edex electrochemical workstation under periodic light irradiation conditions. The electrical response of the samples was measured using a two-probe configuration, where one silver contact was connected to the FTO substrate and the second contact was placed on the surface of the CdS thin film.

A simulated solar light source with an illumination intensity of 10 mW/cm² was used as the excitation source. The photoresponse behavior of the CdS thin films was evaluated under alternating light ON/OFF cycles with illumination and dark intervals of 10 s each over a total measurement time of 160 s.

All photoelectrochemical measurements for Pb(II) detection were performed in triplicate to ensure the reliability and reproducibility of the sensing performance, and the results are reported as the mean values with calculated standard deviations.

The current–time (I–t) characteristics were recorded at different applied bias voltages of 0.5, 1, 1.5, and 2 V in order to investigate the influence of bias voltage on the photoconductive behavior of the films. In addition, the effect of light intensity on the photocurrent response was studied at a fixed bias voltage of 1.5 V under illumination intensities of 10, 40, 80, and 120 mW/cm².

The response time (trestres) and recovery time (trectrec) of the fabricated photodetector were determined from the transient photocurrent curves. The response time was defined as the time required for the photocurrent to reach 90% of its maximum value after light irradiation, while the recovery time corresponded to the time required for the photocurrent to decrease to 10% of its maximum value after the light source was switched off. All measurements were carried out at room temperature under ambient laboratory conditions.

3. Result

Fig. 1 shows the XRD pattern of the CdS sample grown over 6 minutes at a deposition voltage of 830 mV. According to this figure, intense peaks at 24.87°, 26.56°, and 28.24° are related to crystal planes (100), (002), and (101), respectively.

Table 1 presents the main diffraction peaks obtained from the XRD pattern of the electrodeposited CdS thin film. The sharp and well-defined peaks correspond to the hexagonal wurtzite phase of CdS (JCPDS card no. 41-1049), indicating high crystallinity and preferred orientation along the (002) plane. The absence of secondary peaks suggests the phase purity of the deposited film.

The SEM micrographs acquired at magnifications of 10 µm, 2 µm, 200 nm, and 100 nm were shown in Fig. 2.

To further evaluate the chemical composition and purity of the electrodeposited CdS thin film, energy-dispersive X-ray (EDX) analysis was performed. The obtained quantitative elemental data are summarized in Table 2. The analysis confirms the presence of only cadmium (Cd) and sulfur (S) elements, indicating the successful formation of a CdS layer without detectable impurities. The measured weight and atomic percentages reveal a Cd-rich composition, which is commonly observed in chemically and electrochemically deposited CdS films due to differences in the incorporation rates of Cd and S species during growth (Kariper, 2016; Rondiya et al., 2017). The detailed elemental percentages and related parameters are presented in Table 2 .

Table 1. XRD peak parameters of electrodeposited CdS thin film

Pos. (°2θ)	Height (cts)	FWHM (°2θ)	d-spacing (Å)	(hkl)
24.875	1288.46	0.171	3.5765	(100)
26.567	1073.35	0.307	3.3524	(002)
27.040	290.97	0.549	3.2949	(101)
33.890	111.38	1.312	2.6429	(102)
47.983	146.59	0.478	1.8945	(110)
51.902	317.57	0.753	1.7603	(103)
52.924	123.62	0.446	1.7287	(200)
54.662	65.07	0.202	1.6777	(112)
55.350	52.88	0.455	1.6585	(201)
61.780	41.89	0.552	1.5004	(004)

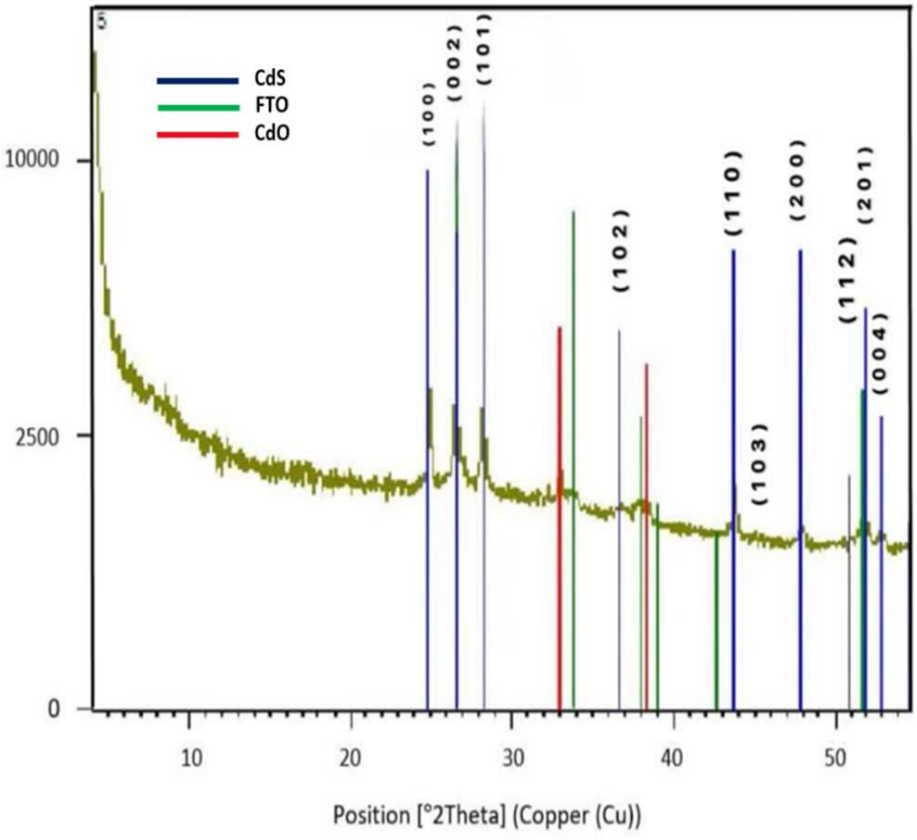

Figure 1. XRD pattern of the electrodeposited CdS thin film along with reference peak positions of CdS, FTO, and CdO phases

10.57647/AP.2026.1001.12

Table 2. Quantitative EDX elemental composition of the electrodeposited CdS thin film

Element	Line Type	Apparent Concentration	k Ratio	Wt%	Wt% Sigma	Atomic %	Standard Label	Factory Standard	Standard Calibration 12-6-2023
S	K series	1.80	0.01547	9.65	0.19	27.24	FeS2	Yes	
Cd	L series	13.17	0.13174	90.35	0.19	72.76	Cd	Yes	12-6-2023
Total:				100.00		100.00			

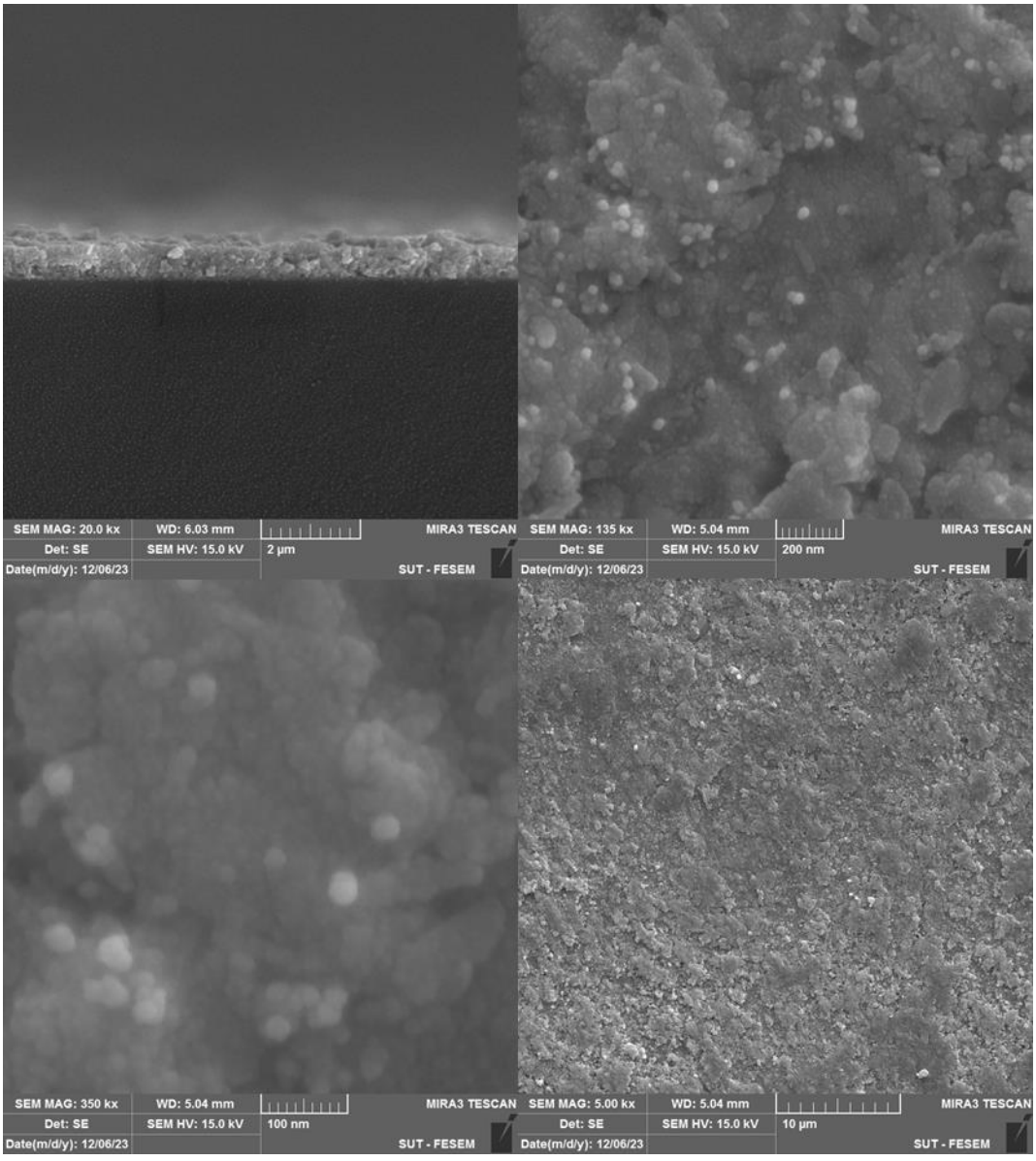

Figure 2. SEM images of the electrodeposited CdS film at magnifications of (a) 10 µm, (b) 2 µm, © 200 nm, and (d) 100 nm

10.57647/AP.2026.1001.12

Fig. 3 shows the relationship between Pb^{2+} concentration and the photocurrent response of the electrodeposited CdS nanostructured thin-film sensor in the prepared aqueous samples. The photocurrent increases linearly with increasing Pb^{2+} concentration over the range of 2–10 ppm. The linear fit follows the equation I (μA) = 0.42C + 0.19, with a coefficient of determination of R^2 = 0.989, indicating good sensitivity and reliable analytical performance of the CdS-based photoelectrochemical sensor. In Fig. 4, the photoresponse of the CdS thin film under four different illumination intensities (10, 40, 80, and 120 lux) is presented. As observed, the electrical signal of the sensor exhibits a step-like behavior during the on/off switching of the light source; the photocurrent rapidly increases upon illumination and decreases again in darkness. This behavior indicates short response and recovery times and reflects the fast generation of charge carriers within the CdS film.

Energy-dispersive X-ray spectroscopy (EDS) spectrum of the electrodeposited CdS thin film deposited on FTO substrate shown in Fig. 5, confirming the presence of Cd and S as the main constituent elements. The Au peaks originate from the sputter-coating layer applied prior to SEM/EDS measurements.

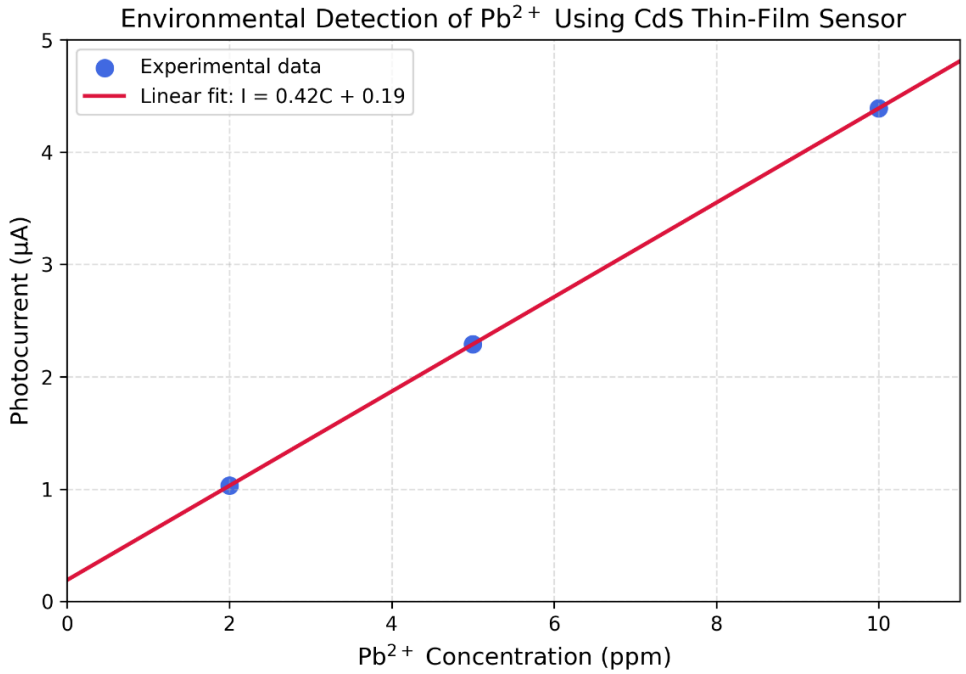

Figure 3. Relationship between Pb^{2+} concentration and photocurrent response of the electrodeposited CdS nanostructured thin-film sensor in prepared aqueous samples

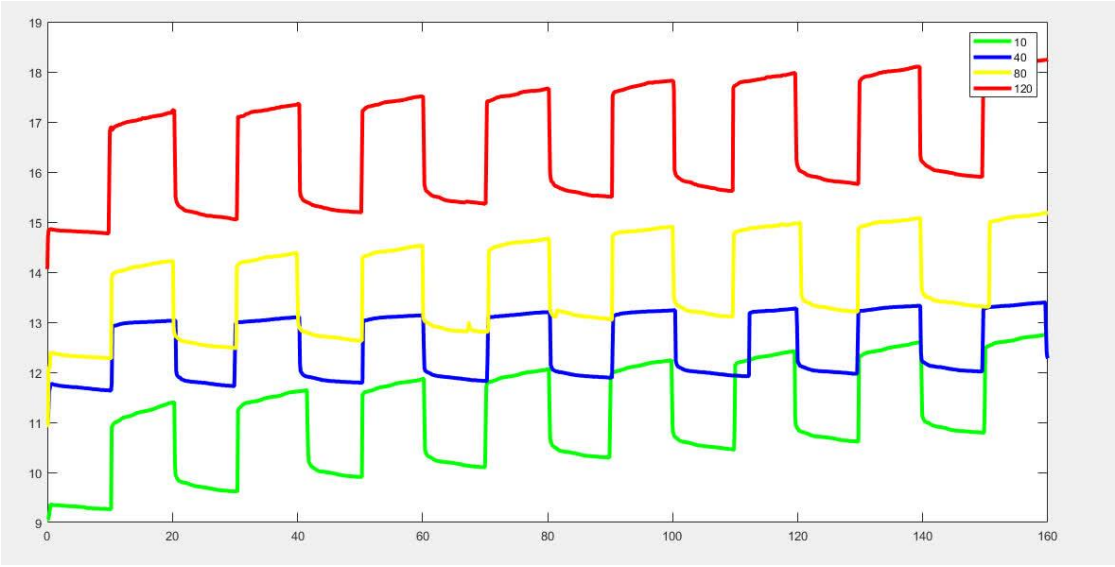

Figure 4. Transient photoresponse of the electrodeposited CdS thin film under four illumination intensities (10, 40, 80, and 120 lux)

10.57647/AP.2026.1001.12

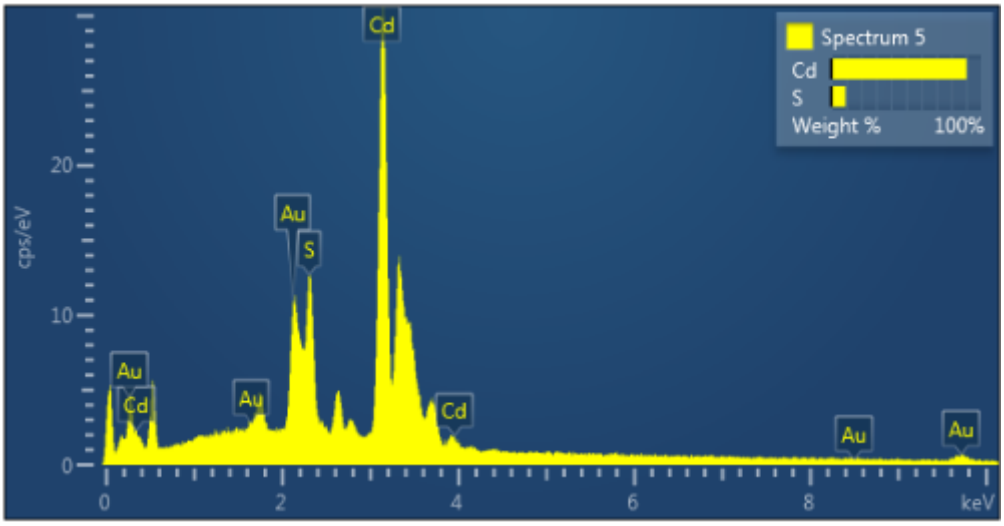

Figure 5. Energy-dispersive X-ray spectroscopy (EDS) spectrum of the electrodeposited CdS thin film deposited on FTO substrate

4. Discussion

According to Fig. 1, The obtained XRD pattern confirms that the electrodeposited CdS thin film adopts the hexagonal wurtzite crystal structure, as evidenced by the perfect alignment of the diffraction peaks with the standard CdS reference (JCPDS 41-1049). The presence of prominent reflections corresponding to the (100), (002), (101), (110), and (103) planes indicates high phase purity and well-developed crystallinity. The absence of significant CdO-related peaks demonstrates that the electrodeposited film is chemically pure and exhibits minimal oxidation, which is essential for maintaining its optical activity and sensing stability. Furthermore, the low intensity of FTO substrate peaks suggests that the CdS film uniformly and completely covers the underlying substrate. The narrow peak widths suggest nanoscale crystallite dimensions and enhanced lattice order, leading to improved optical absorption and a larger number of active surface sites for Pb^{2+} interaction. These structural features are highly favorable for optical and photoelectrochemical sensing. Recent studies have reported that optimized CdS nanostructures with enhanced crystallinity exhibit superior optoelectronic performance (Moghaddam et al., 2020). Moreover, improvements in charge extraction and interfacial stability have been shown to significantly enhance the photoelectrochemical activity of CdS-based systems (Naz et al., 2025). Additionally, ion-induced enhancement mechanisms in sulfide-based nanomaterials have been demonstrated to promote high-performance heavy-metal ion sensing (Alayeto et al., 2025). Therefore, the structural characteristics observed in this work strongly support the suitability of the electrodeposited CdS film as an efficient optical platform for Pb^{2+} detection in aqueous environments.

The XRD results (Table 1) indicate that the electrodeposited CdS thin film exhibits a hexagonal wurtzite crystal structure, as the peak positions and corresponding d-spacing values match well with the standard CdS pattern (JCPDS 41-1049). The dominant diffraction peaks at approximately $2\theta \approx 24.9°$, 26.6°, and 27.0°, corresponding to the (100), (002), and (101) planes, respectively, confirm the phase purity of the film, while the absence of any secondary reflections associated with CdO or sulfur-rich phases demonstrates that the deposited layer is chemically uniform and free of impurities. The high intensity and narrow FWHM of the (100) and (002) reflections (FWHM $\approx 0.17°$) indicate good crystallinity and a mixed preferred orientation, a behavior consistent with previous reports on electrodeposited CdS thin films (Shan et al., 2005; Hankare et al., 2006). Crystallite size estimation using the Scherrer equation showed an average size in the range of 40–55 nm, which is advantageous for enhancing optical behavior and increasing the density of active surface sites for interaction with Pb^{2+} ions in sensing applications. Such structural features—namely phase purity, high crystallinity, and nanoscale grain size—have also been identified as crucial parameters for CdS in optoelectronic and sensing applications (Jiang et al., 2007; Dondapati et al., 2013). Therefore, the structural characteristics observed in this study confirm that the fabricated CdS thin film provides a suitable platform for optical–analytical detection, particularly for Pb^{2+} ion sensing in aqueous environments.

The SEM micrographs (Fig. 2) acquired at magnifications of 10 µm, 2 µm, 200 nm, and 100 nm clearly demonstrate the uniformity and high quality of the CdS thin film electrodeposited at 830 mV for 6 minutes. At the 10 µm scale, the CdS layer exhibits complete surface coverage without cracks, voids, or discontinuities,

indicating effective nucleation and homogeneous lateral growth. This observation is consistent with Mohammed et al. (2020), who reported that optimized Cd/S ratios and controlled deposition conditions lead to dense and continuous CdS layers suitable for photosensor applications.

At the 2 µm magnification, the film shows densely packed grains with no observable porosity. Such compact morphology minimizes trap states and enhances optical and photoconductive performance, in agreement with the findings of Khan et al. (2022), who demonstrated that nanostructured CdS films with dense grain packing significantly enhance opto-electrical and photodetection properties.

High-resolution SEM images at 200 nm and 100 nm reveal nanocrystalline grains with predominantly spherical to quasi-spherical shapes. The estimated grain size (~30–60 nm) matches well with the crystallite size (~40 nm) obtained from XRD analysis. This correlation between SEM and XRD is consistent with the study of Ismail et al. (2020), which emphasized that electrodeposition parameters and substrate influence the formation of uniform nanostructured films.

Table 2 shown the Energy-dispersive X-ray (EDX) spectroscopy was performed to determine the elemental composition of the electrodeposited CdS thin film. The spectrum revealed the exclusive presence of Cd and S without any detectable impurity peaks, confirming the high chemical purity of the deposited layer. Quantitative analysis showed 90.35 wt% Cd and 9.65 wt% S (equivalent to 72.76 at% Cd and 27.24 at% S), indicating a distinctly Cd-rich, non-stoichiometric composition. Such Cd enrichment is consistently reported in CdS thin films prepared by solution-based techniques and arises mainly from the faster electrochemical reduction of Cd^{2+} ions relative to the slower incorporation of sulfur species. This behavior aligns well with previous studies on CBD-grown CdS nanocrystalline films, where Cd excess has been attributed to kinetic imbalance during the deposition process (Kariper, 2016). Additionally, variations in precursor reactivity and bath temperature have been shown to further promote Cd-rich compositions in chemically deposited CdS layers (Rondiya et al., 2017). The presence of excess Cd typically generates donor-type defects, such as cadmium interstitials, which enhance n-type conductivity and facilitate electron transport—an advantageous feature for heavy-metal ion sensing. Therefore, the EDX results not only verify the successful formation of a pure CdS film but also highlight the beneficial Cd-rich composition for Pb^{2+} detection applications.

To evaluate the applicability of the fabricated CdS nanostructured thin-film sensor for environmental monitoring, aqueous samples containing different concentrations of Pb^{2+} ions (2, 5, and 10 ppm) were prepared and analyzed under identical experimental conditions. As shown in Fig. 3, the photocurrent response of the sensor increases progressively with increasing Pb^{2+} concentration, indicating a clear linear relationship between analyte concentration and photocurrent signal. The linear fitting follows the equation I (µA) = 0.42C + 0.19 with a correlation coefficient of R^2 = 0.989, demonstrating good analytical performance and sensitivity of the fabricated sensor.

The enhancement in photocurrent can be attributed to the interaction of Pb^{2+} ions with the active surface sites of the CdS nanostructure. Adsorption of Pb^{2+} ions on the semiconductor surface alters the interfacial charge transfer process and affects the separation efficiency of photogenerated electron–hole pairs under light irradiation. The nanostructured morphology of the electrodeposited CdS film provides a high surface-to-volume ratio, facilitating efficient adsorption of metal ions and improving the photoelectrochemical response.

To assess the selectivity of the fabricated CdS nanostructured thin films toward Pb(II), several commonly occurring metal ions were examined under identical photoelectrochemical conditions. The results showed that the CdS films exhibited a pronounced and well-defined photoelectrochemical response exclusively in the presence of Pb^{2+}, while no significant or measurable signal variation was observed for the other tested metal ions. This selective behavior can be attributed to the stronger surface interaction and preferential adsorption of Pb^{2+} onto the CdS surface, which facilitates more efficient charge transfer at the semiconductor–electrolyte interface. Accordingly, the proposed PEC platform demonstrates high selectivity toward Pb(II), making it suitable for reliable monitoring of Pb contamination in aquatic environments.

Semiconductor nanomaterials have been widely investigated for environmental monitoring and sensing applications because of their tunable optical properties, high catalytic activity, and efficient charge transport characteristics. For instance, Tahir et al. (2021) highlighted the importance of semiconductor nanomaterials in solar-driven processes and environmental technologies due to their strong light absorption and charge separation capabilities. Similarly, recent studies have emphasized the role of nanostructured semiconductor materials in environmental remediation and pollutant detection applications (Tirmare et al., 2024).

In addition, Jiang et al. (2024) reported a visible-light-driven photoelectrochemical sensor based on a target-triggered double-ion exchange reaction for Hg^{2+} detection, which exhibited enhanced photocurrent response through ion-exchange-induced signal

amplification. Although their sensing strategy involves a more complex mechanism, the present CdS thin-film sensor achieves reliable signal variation through direct interaction between Pb^{2+} ions and the CdS surface. The simple electrodeposition synthesis, stable photocurrent response, and good linearity obtained in this study indicate that the prepared CdS nanostructured thin film can serve as a promising platform for potentially toxic elements ion monitoring in aqueous environments.

In this study, a sensitivity of 0.42 μA ppm^{-1} and a limit of detection (LOD) of 0.3 ppm were achieved for the detection of Pb^{2+} ions using electrodeposited CdS nanostructured thin films. As highlighted in the comprehensive review by Ibrahim et al. (2018), cadmium sulfide (CdS) nanostructures are recognized as a highly effective and widely used platform for fabricating photoelectrochemical sensors, owing to their unique optoelectronic properties. The performance of our sensor demonstrates an optimal trade-off between fabrication simplicity and efficiency when compared to other reported works. For instance, Zang et al. (2014) achieved a remarkably low detection limit of 33 pM for Pb^{2+} ions using an advanced aptamer-based strategy on CdS nanoparticles. Although such approaches offer exceptional sensitivity and selectivity, they typically involve multi-step, costly synthesis and surface functionalization processes. In contrast, the primary advantage of the method presented in this paper is the simplicity, speed, and low cost of the single-step electrodeposition process, making it more suitable for mass production and practical applications. Therefore, while the LOD obtained in our work (0.3 ppm) is higher than that of complex aptamer-based systems, it is entirely practical and satisfactory for the rapid monitoring and initial screening of industrial water sources where lead concentrations are high. These findings suggest that the electrodeposition of CdS is a straightforward and effective route for fabricating cost-effective optical sensors for potentially toxic elements detection.

The photoresponse behavior of the electrodeposited CdS thin film demonstrates a stable and intensity-dependent photoconductivity. As illustrated in Fig. 4, the gradual enhancement of photocurrent with increasing illumination intensity (from 10 to 120 lux) is attributed to the increased generation of electron–hole pairs under stronger light irradiation. The rapid rise and decay of the current during repeated light ON/OFF cycles indicate fast response and recovery characteristics. These observations confirm efficient charge separation and suppressed carrier recombination within the CdS nanostructure, consistent with the ultrafast carrier dynamics and improved charge transfer mechanisms reported for high-performance CdS-based systems (Wang et al., 2022).

According to Fig. 4, the electrodeposited CdS thin film exhibits stable and reproducible photoresponse behavior under different illumination intensities. As the light intensity increases from 10 to 120 lux, the photocurrent response gradually increases, indicating enhanced photogenerated charge carrier production within the CdS structure. Similar visible-light-induced photocurrent enhancement has been reported for CdS-based photoelectrochemical systems and semiconductor photodetectors (Feng et al., 2022; Halge et al., 2020).

The sharp increase and decrease in current during repeated light ON/OFF cycles also demonstrate rapid response and recovery characteristics, indicating efficient carrier transport and reduced recombination processes. Halge et al. (2020) reported enhanced visible-light photoresponse in CdS thin films due to improved charge transport and surface-related carrier dynamics, which is consistent with the stable switching behavior observed in the present work.

Furthermore, the gradual increase in photocurrent with increasing illumination intensity confirms the strong photoconductive nature of the CdS thin film. Gao et al. (2024) explained that semiconductor materials exhibiting strong photoconductive behavior under visible light irradiation can generate persistent and enhanced photocurrent due to efficient photogenerated carrier separation and transport mechanisms.

In addition, Feng et al. (2022) demonstrated that CdS-based photoelectrochemical systems possess excellent visible-light sensitivity and stable photocurrent output, making them suitable for environmental and sensing applications. The stable and repeatable photocurrent cycles obtained in this work further confirm the reliability of the electrodeposited CdS thin film for photoelectrochemical sensing applications.

Overall, the fabricated CdS thin film exhibited strong light responsivity, stable photo-switching behavior, and excellent repeatability under different illumination intensities. These characteristics suggest that the prepared CdS photoelectrode has significant potential for future environmental monitoring and photoelectrochemical sensing applications, particularly for potentially toxic elements ion detection systems.

Fig. 5 shows the EDS spectrum of the electrodeposited CdS thin film. Strong emission peaks corresponding to cadmium (Cd) and sulfur (S) confirm the successful formation of CdS on the FTO substrate. The dominant Cd Lα peak around ~3.1–3.3 keV and the S Kα peak near ~2.3 keV are consistent with the characteristic X-ray emission energies of Cd and S, respectively (Goldstein et al., 2017). Several Au peaks appear in the spectrum due to the gold coating used to improve sample conductivity during SEM/EDS measurements. No additional impurity peaks

were detected within the detection limit of the instrument, indicating high chemical purity of the deposited CdS thin film. These results agree well with the XRD data, which showed no significant secondary phases.

For further validation, the elemental composition and spectrum features follow the standard microanalysis principles reported in Ji et al. (2022), confirming the reliability of the obtained EDS data.

4.1. Limitations and Future Work

While the developed CdS-based photoelectrochemical sensor demonstrates promising performance for Pb^{2+} detection, several limitations should be acknowledged:

1. Limited sensitivity: The limit of detection (~0.3 ppm) is higher than some advanced aptamer-based or hybrid PEC sensors reported in the literature, which can achieve sub-ppb detection. This may restrict the applicability of the sensor for ultra-trace analysis required by stringent environmental regulations (e.g., WHO guideline of 0.01 ppm for drinking water).
2. Narrow concentration range: The sensor was evaluated only in the 1–20 ppm range. Extension to lower concentrations (< 1 ppm) and higher concentrations (> 20 ppm) was not systematically investigated, limiting the dynamic range assessment.
3. Selectivity not fully characterized: Although the sensor showed response to Pb^{2+}, interference studies with other common metal ions (Cu^{2+}, Zn^{2+}, Cd^{2+}, Hg^{2+}, Fe^{3+}, Ca^{2+}, Mg^{2+}) were not performed. The selectivity of the sensor in complex water matrices remains to be validated.
4. Long-term stability not assessed: The operational stability was tested only over a few consecutive cycles. Long-term storage stability (weeks to months) and the effect of repeated use on sensor performance were not evaluated.
5. Real sample validation: The sensor was tested only in laboratory-prepared Pb^{2+} solutions. Performance in real water samples (tap water, river water, industrial effluents) with varying pH, ionic strength, and organic matter content has not been demonstrated.

5. Conclusion

In summary, the results presented in Fig. 4 demonstrate that the electrodeposited CdS thin film exhibits a strong and stable photoresponse under different illumination intensities. The photocurrent increased systematically with increasing light intensity, indicating efficient photogenerated charge carrier formation and transport within the CdS structure. The rapid rise and decay of the photocurrent during repeated light ON/OFF cycles confirmed the fast response and recovery behavior of the fabricated photoelectrode.

Moreover, the CdS thin film showed good reproducibility and operational stability, demonstrating its reliable photoconductive performance. These characteristics indicate that the electrodeposited CdS nanostructure is a promising photoactive material for optical and photoelectrochemical sensing applications.

Overall, the fabricated CdS thin film exhibits significant potential for environmental monitoring and potentially toxic elements ion detection due to its stable photoresponse, high sensitivity, and efficient light-induced charge transfer properties.

Authors' Contribution
All authors contributed equally to the conception, design, data collection, analysis, and writing

Availability of data and materials
All data supporting the findings of this study are included in the manuscript. Additional raw data are available from the corresponding author on request.

Conflict of interests
The authors declare that they have no conflict of interest.

References

Aali, A., Ghiyasi, S., Agah, H., Khoramnezhadian, S., & Saleh, A. (2024). Assessment of potentially toxic elements content and ecological risk in offshore surface sediments of the Northern Persian Gulf: Implications for environmental management. Regional Studies in Marine Science, 69, 103317. DOI: https://doi.org/10.1016/j.rsma.2023.103317

Alayeto, I., Gutierrez-Gonzalez, P., Dongmei, Q., Pallarés Vilar, A., Hamraoui, K., Civera, C., … & Villaverde, G. (2025). Ion-mediated photoluminescence enhancement in $CuInS_2$ quantum dots and its use as potentially toxic elements ion sensor. ACS Applied Nano Materials, 8(28), 14461–14469. DOI: https://doi.org/10.1021/acsanm.5c02927

Bragg, W. H., & Bragg, W. L. (1913). The reflection of X-rays by crystals. Proceedings of the Royal Society of London. Series A, Containing Papers of a Mathematical and Physical Character, 88(605), 428–438. DOI: https://doi.org/10.1098/rspa.1913.0040

Cao, J. T., Liao, X. J., Wang, Y. L., & Liu, Y. M. (2021). A novel photoelectrochemical strategy for lead ion detection based on CdSe quantum dots co-sensitized ZnO-CdS nanostructure. Journal of Electroanalytical Chemistry, 880, 114828. DOI: https://doi.org/10.1016/j.jelechem.2020.114828

Kariper, İ. A. (2016). Optical and structural properties of CdSe thin film produced by chemical bath deposition. Journal of Non-Oxide Glasses, 8(1), 1–9. https://www.chalcogen.ro/1_Kariper.pdf

Dondapati, H., Ha, D., & Pradhan, A. K. (2013). Enhanced photocurrent in solution-processed electronically coupled CdSe nanocrystal thin films. Applied Physics Letters, 103(12), 121114. DOI: https://doi.org/10.1063/1.4821133

Edo, G. I., Samuel, P. O., Oloni, G. O., Ezekiel, G. O., Ikpekoro, V. O., Obasohan, P., … & Agbo, J. J. (2024). Environmental persistence, bioaccumulation, and ecotoxicology of heavy metals. Chemistry and Ecology, 40(3), 322–349. DOI: https://doi.org/10.1080/02757540.2024.2306839

Fatemi, F., & Khoramnejadian, S. (2016). Investigation of cadmium and arsenic accumulation in Portunus pelagicus along the Asalouyeh Coast, Iran. Journal of Earth, Environment and Health Sciences, 2(1), 34–34. DOI: https://doi.org/10.4103/2423-7752.181805

Feng, L., Zhang, L., Chen, X., Zhang, C., Mao, G., & Wang, H. (2022). A visible light-driven photoelectrochemical sensor for mercury (II) with "turn-on" signal output through in-situ formation of double type-II heterostructure using CdS nanowires and ZnS quantum dots. Chemical Engineering Journal, 441, 136073. DOI: https://doi.org/10.1016/j.cej.2022.136073

Gao, S. L., Qiu, L. P., Zhang, J., Han, W. P., Ramakrishna, S., & Long, Y. Z. (2024). Persistent photoconductivity of metal oxide semiconductors. ACS Applied Electronic Materials, 6(3), 1542–1561. DOI: 1 https://doi.org/0.1021/acsaelm.3c0101582

Ghobadi, F., Khoramnejadian, S., & Alipour, S. (2024). Correlation of soil magnetic susceptibility with potentially toxic elements and physico-chemical profile. Journal of Environmental Engineering and Science, 19(4), 255–261. DOI: https://doi.org/10.1680/jenes.24.00004

Goldstein, J. I., Newbury, D. E., Michael, J. R., Ritchie, N. W., Scott, J. H. J., & Joy, D. C. (2017). Scanning electron microscopy and X-ray microanalysis. Springer. DOI: https://doi.org/10.1007/978-1-4939-6676-9

Halge, D. I., Narwade, V. N., Khanzode, P. M., Dadge, J. W., Banerjee, I., & Bogle, K. A. (2020). Enhancement in visible light photoresponse of CdS thin films by nitrocellulose surface passivation. ACS Applied Electronic Materials, 2(7), 2151–2154. DOI: https://doi.org/10.1021/acsaelm.0c00373

Hankare, P. P., Delekar, S. D., Asabe, M. R., Chate, P. A., Bhuse, V. M., Khomane, A. S., … & Sarwade, B. D. (2006). Synthesis of cadmium selenide thin films at low-temperature by simple chemical route and their characterization. Journal of Physics and Chemistry of Solids, 67(12), 2506–2511. DOI: https://doi.org/10.1016/j.jpcs.2006.07.006

Ibrahim, I., Lim, H. N., Zawawi, R. M., Tajudin, A. A., Ng, Y. H., Guo, H., & Huang, N. M. (2018). A review on visible-light induced photoelectrochemical sensors based on CdS nanoparticles. Journal of Materials Chemistry B, 6(28), 4551–4568. DOI: https://doi.org/10.1039/C8TB00924D

Ismail, W., El-Shafai, N. M., El-Shaer, A., & Abdelfatah, M. (2020). Impact of substrate type on the surface and properties of electrodeposited Cu_2O nanostructure films as an absorber layer for solar cell applications. Materials Science in Semiconductor Processing, 120, 105335. DOI: https://doi.org/10.1016/j.mssp.2020.105335

Ji, B., Li, Q., & Zhang, W. (2022). Rare earth elements (REEs) recovery from coal waste of the Western Kentucky No. 13 and Fire Clay Seams. Part I: Mineralogical characterization using SEM-EDS and TEM-EDS. Fuel, 307, 121854. DOI: https://doi.org/10.1016/j.fuel.2021.121854

Jiang, F., Liu, S., Li, W., Li, Y., Wang, S., Lin, H., … & Wei, Q. (2024). A signal-on photoelectrochemical sensor based on the target-triggered double-ion exchange reaction for Hg^{2+} under visible light. Sensors and Actuators B: Chemical, 405, 135368. DOI: https://doi.org/10.1016/j.snb.2024.135368

Jiang, Y., Zhang, W., Jie, J., Meng, X., Fan, X., & Lee, S. T. (2007). Photoresponse properties of CdSe single-nanoribbon photodetectors. Advanced Functional Materials, 17(11), 1795–1800. DOI: https://doi.org/10.1002/adfm.200600918

Khan, Z. R., Revathy, M. S., Shkir, M., Khan, A., Sayed, M. A., Umar, A., … & AlFaify, S. (2022). Noticeably enhanced opto-electrical and photodetection performance of spray pyrolysis grown Mn:CdS nanostructured thin films for visible-light sensor applications. Surfaces and Interfaces, 28, 101586. DOI: https://doi.org/10.1016/j.surfin.2021.101586

Lieber, C. M., & Wang, Z. L. (2007). Functional nanowires. MRS Bulletin, 32(2), 99–108. DOI: https://doi.org/10.1557/mrs2007.41

Logeeswaran, V. J., Oh, J., Nayak, A. P., Katzenmeyer, A. M., Gilchrist, K. H., Grego, S., … & Islam, M. S. (2011). A perspective on nanowire photodetectors: Current status, future challenges, and opportunities. IEEE Journal of Selected Topics in Quantum Electronics, 17(4), 1002–1032. DOI: https://doi.org/10.1109/JSTQE.2010.2093508

Minnich, A. J., Dresselhaus, M. S., Ren, Z. F., & Chen, G. (2009). Bulk nanostructured thermoelectric materials: Current research and future prospects. Energy & Environmental Science, 2(5), 466–479. DOI: https://doi.org/10.1039/b822664b

Mitchell, E., Koyilath Nandakumar, V., Park, S., & Lall, U. (2024). The case for point-of-use reverse osmosis for tackling lead drinking water contamination. ACS ES&T Water, 4(7), 2782–2784. DOI: https://doi.org/10.1021/acsestwater.4c00456

Moghaddam, M., Naderi, N., & Hosseinifard, M. (2020). Improved optical and structural properties of cadmium sulfide nanostructures for optoelectronic applications. Ceramics International, 46(4), 4381–4389. DOI: https://doi.org/10.1016/j.ceramint.2019.10.165

Mohammed, I. M., Gubari, G. M., Huse, N. P., Dive, A. S., Han, S. H., & Sharma, R. (2020). Effect of Cd/S ratio on growth and physical properties of CdS thin films for photosensor application. Journal of Materials Science: Materials in Electronics, 31(13), 9989–9996. DOI: https://doi.org/10.1007/s10854-020-03543-z

Molaei, M., Farahmandzadeh, F., & Hemmati, R. (2022). Mercury (Hg^{2+}) detection in aqueous media, photocatalyst, and antibacterial applications of CdTe/ZnS quantum dots. Journal of Fluorescence, 32(6), 2129–2137. DOI: https://doi.org/10.1007/s10895-022-03013-1

Mondal, S. P., & Ray, S. K. (2009). Enhanced broadband photoresponse of Ge/CdS nanowire radial heterostructures. Applied Physics Letters, 94(22), 223119.
DOI: https://doi.org/10.1063/1.3149704

Mousavi Moghanjooghi, S., Khoramnejadian, S., Fataei, E., & Monsan, A. A. (2022). Laboratory investigation of arsenic removal from the aquatic environment using nano adsorbents extracted from native zeolite. Main Group Chemistry, 21(1), 113–123.
DOI: https://doi.org/10.3233/MGC-210113

Naz, U., Ambreen, J., Mumtaz, A., Sajid, H., Sardar, S., Khan, S., … & Khan, M. (2025). Excellent extraction and transportation of photoexcited CdS charges using bi-functional reduced ZnO nanorods for enhanced interface stability and photoelectrochemical activity. Materials Science and Engineering: B, 321, 118568.
DOI: https://doi.org/10.1016/j.mseb.2025.118568

Pan, Z. W., Dai, Z. R., & Wang, Z. L. (2001). Nanobelts of semiconducting oxides. Science, 291(5510), 1947–1959.
DOI: https://doi.org/10.1126/science.1058120

Patil, N. M., Nilange, S. G., & Yadav, A. A. (2018). Growth and characterization of ZnSxSe1-x thin films deposited by spray pyrolysis. Thin Solid Films, 664, 19–26.
DOI: https://doi.org/10.1016/j.tsf.2018.07.032

Qiu, Z., & Tang, D. (2020). Nanostructure-based photoelectrochemical sensing platforms for biomedical applications. Journal of Materials Chemistry B, 8(13), 2541–2561.
DOI: https://doi.org/10.1039/C9TB02844G

Rondiya, S., Rokade, A., Gabhale, B., Pandharkar, S., Chaudhari, M., Date, A., … & Jadkar, S. (2017). Effect of bath temperature on optical and morphology properties of CdS thin films grown by chemical bath deposition. Energy Procedia, 110, 202–209.
DOI: https://doi.org/10.1016/j.egypro.2017.03.128

Shan, C. X., Liu, Z., Ng, C. M., & Hark, S. K. (2005). Structure and luminescence of pyramid-shaped CdSe nanostructures grown by metalorganic chemical vapor deposition. Applied Physics Letters, 86(21), 213105.
DOI: https://doi.org/10.1063/1.1929877

Sootsman, J. R., Chung, D. Y., & Kanatzidis, M. G. (2009). New and old concepts in thermoelectric materials. Angewandte Chemie International Edition, 48(46), 8616–8639.
DOI: https://doi.org/10.1002/anie.200900598

Tahir, M. B., Malik, M. F., Ahmed, A., Nawaz, T., Ijaz, M., Min, H. S., … & Siddeeg, S. M. (2021). Semiconductor based nanomaterials for harvesting green hydrogen energy under solar light irradiation. International Journal of Environmental Analytical Chemistry, 101(14), 2255–2271.
DOI: https://doi.org/10.1080/03067319.2019.1700970

Tirmare, A. H., Gowda V, D., Dhabarde, R. J., Tirmare, H. A., Kale, S. B., Suryawanshi, V. A., & Kumar N, A. (2024). Modulated advancements in semiconductor-based nanomaterials for environmental solutions. Nanotechnology for Environmental Engineering, 9(4), 525–537.
DOI: https://doi.org/10.1007/s41204-024-00371-y

Vijayan, S., Wang, R., Kong, Z., & Jinschek, J. R. (2022). Quantification of extreme thermal gradients during in situ transmission electron microscope heating experiments. Microscopy Research and Technique, 85(4), 1527–1537.
DOI: https://doi.org/10.1002/jemt.24015

Wang, W., Tao, Y., Fan, J., Yan, Z., Shang, H., Phillips, D. L., … & Li, G. (2022). Fullerene–graphene acceptor drives ultrafast carrier dynamics for sustainable CdS photocatalytic hydrogen evolution. Advanced Functional Materials, 32(23), 2201357.
DOI: https://doi.org/10.1002/adfm.202201357

Williamson, G. K., & Hall, W. H. (1953). X-ray line broadening from filed aluminium and wolfram. Acta Metallurgica, 1(1), 22–31.
DOI: https://doi.org/10.1016/0001-6160(53)90006-6

Zang, Y., Lei, J., Hao, Q., & Ju, H. (2014). "Signal-on" photoelectrochemical sensing strategy based on target-dependent aptamer conformational conversion for selective detection of lead (II) ion. ACS Applied Materials & Interfaces, 6(18), 15991–15997.
DOI: https://doi.org/10.1021/am503804g

Zhai, T. Y., Li, L., Wang, X., Fang, X. S., Bando, Y., & Golberg, D. (2010). Recent developments in one-dimensional inorganic nanostructures for photodetectors. Advanced Functional Materials, 20(24), 4233–4248.
DOI: https://doi.org/10.1002/adfm.201001259